JOURNAL OF SOLID STATE CHEMISTRY 76, 52–63 (1988)

The Crystal Structure and Density of β-Rhombohedral Boron*

G. A. SLACK, C. I. HEJNA, M. F. GARBAUSKAS, AND J. S. KASPER

General Electric Corporate Research and Development, Schenectady, New York 12301

Received November 9, 1987; in revised form March 11, 1988

The crystal structure of three different samples of melt-grown β-rhombohedral boron has been reinvestigated. There are 20 different symmetry-equivalent atomic positions in the unit cell, four of which have not been previously reported. Six of the 20 are partially occupied. The hexagonal unit cell contains a total of 320.1 boron atoms as determined from the electron density. This gives an X-ray-predicted crystal density of 2.333(5) g/cm³ compared to a pycnometric value of 2.333(2) g/cm³. There are local density variations with the large unit cell associated with the partially occupied sites. © 1988 Academic Press, Inc.

I. Introduction

The structure of the high-temperature modification of boron that is in equilibrium with the melt at atmospheric pressure is the β-rhombohedral form. Its atomic structure was first worked out by Hughes *et al.* (*1*). A full report of this work was given by Hoard *et al.* (*2*). Two further refinements were published by Geist *et al.* (*3*) and Callmer (*4*). One of the serious problems with all of these refinements was stated by Hoard *et al.* (*2*) in 1970: The X-ray studies found 315 boron atoms per hexagonal cell while the observed density corresponded to 324 atoms per unit cell. The difference was unexplained in any of these studies except for the suggestion by Hoard *et al.* that disorder and partial occupancy of the boron sites may play a role. Callmer (*4*) stated that in his sample, in which he found 16 occupied sites, any unreported boron sites were less than 7% occupied.

II. Experimental

Sample Preparation and Purity

Three different single-crystal samples were studied by X-ray techniques; all were grown from the melt. Two of them were grown in this laboratory from high purity boron powder melted in a CVD boron nitride crucible in an argon atmosphere. The boron powder was zone-refined first by Eagle Picher Laboratories (Miami, OK). One of these samples, MG57, was cooled rapidly from the melting temperature at a cooling rate of about 350°C/min. The second, MG179, was slowly cooled from the melt at a rate of about 2.2°C/min. These were grown in 1982 and 1985, respectively, and have been at room temperature since then. These samples were about 0.04 cm in their largest dimension when measured. The third sample was grown by Eagle Picher

* This study was supported in part by the U.S. Department of Energy on Contract DE-AC01-81NE32084.

0022-4596/88 $3.00

TABLE I

ELECTRICAL CONDUCTIVITY, σ, AT ROOM TEMPERATURE AND ESTIMATED CARBON CONTENT OF β-BORON CRYSTALS

Sample	σ (mho/cm)	Carbon (atom %)	Carbon atoms per hexagonal unit cell
MG57	8.3×10^{-7}	6×10^{-2}	0.2
MG179	3.8×10^{-7}	3×10^{-2}	0.1
EP	1.4×10^{-7}	1×10^{-2}	0.03

Research Laboratories in 1974 using an electron-beam-heated floating-zone process. We studied a small cube 0.03 cm on an edge cut from a 2.4-cm-long, 0.6-cm-diameter single-crystal rod. This crystal had also been residing at room temperature since it was grown. All of the crystals were shiny grey in color corresponding to a semiconductor with an intrinsic band gap of 1.6 eV.

In all cases, the purity of the starting boron material was at least four-nines pure; the dominant impurity was residual carbon. For the two samples grown in BN there was some residual nitrogen in the range 30 to 200 atomic ppm. In order to check for the residual carbon in the grown crystal boules, we measured the room-temperature electrical conductivity. The results are shown in Table I. Using the electrical conductivity we can refer to Fig. 1 in order to estimate the carbon content. The results are given in Table I.

Figure 1 was constructed from the published data of Cueilleron *et al.* (*5*) (open circles) and polycrystalline carbon-doped samples grown in the present series of experiments (filled circles). The present carbon-doped samples had a grain size of about 0.1 cm, whereas those of Cueilleron *et al.* had a grain size of about 0.01 cm. In our series of electrical conductivity experiments we have found that Al, Ca, Mg, Si, and O impurities have a much smaller effect on the electrical conductivity, σ, than do C or Fe. Thus we have neglected the effects of these in Cueilleron's samples. We have found that Fe impurities do have an effect of σ comparable to carbon, but the Fe content in their samples was generally small enough to be ignored. Thus to the accuracy needed in Fig. 1 the carbon content in Cueilleron's samples determines σ. The horizontal line at the bottom of Fig. 1 is the σ of undoped, intrinsic β-boron. A carbon content of ≤20 ppm is needed to reach this, a value well below that found in any of the present samples.

The electrical σ data show that the carbon content of the present samples is low, ranging from 100 to 600 atomic ppm. Analyses supplied by Eagle Picher Laboratories state that the crystals grown by the electron beam floating-zone process had typical impurity contents of:

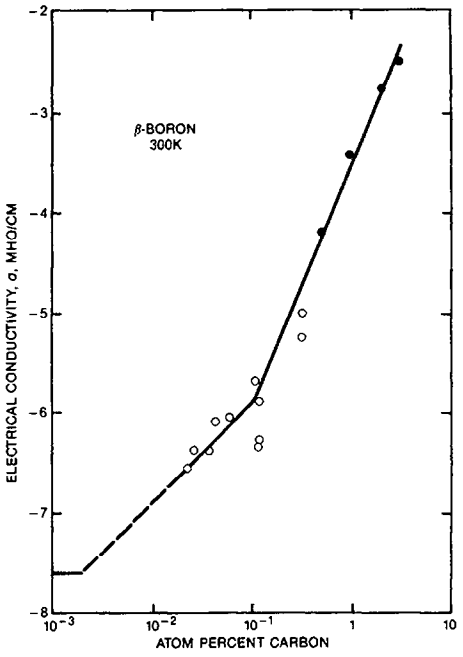

FIG. 1. The room-temperature electrical conductivity of polycrystalline β-boron as a function of carbon content. The open circles are from Ref. (*5*); the filled circles are the present data.

Oxygen	6 atom ppm
Carbon	150 atom ppm.

The zone-refined powder from which samples MG57 and MG179 were grown had aproximate impurity contents of:

Silicon	2 atom ppm
Magnesium	5 atom ppm
Carbon	1750 atom ppm.

From Table I we see that our melt-grown samples were somewhat lower in carbon than the starting material. In any case the dominant impurity is carbon, but there is no more than 0.2 carbon atom in the hexagonal unit cell of β-boron which contains ~320 boron atoms. This amount of carbon is not sufficient to influence our crystal structure results.

Pycnometric Density

The pycnometric density of several different samples of boron was measured by making a liquid mixture in which the crystals neither floated nor sank. The density of this liquid was measured by weighing a known volume in a previously calibrated glass pycnometer bottle. For most samples a mixture of 1,2-dibromethane and 1,1,2,2-tetrabromoethane held at 23°C was used. For the isotopically enriched ^{10}B samples a lower density mixture of 1,2-dibromoethane and bromotrichloromethane was employed. The estimated accuracy of this method is about ± 0.001 g/cm^3. A similar density-measuring technique was employed by Slack *et al.* (*6*).

X-Ray Structure Refinement

The X-ray structure was determined at room temperature (295 K) using an automated Nicolet P3F four-circle diffractometer (Nicolet Instrument Corp., Fremont, CA) with monochromatized Mo$K\alpha$ radiation (λ = 0.71069 Å). Data were collected for the $\pm h$, $\pm k$, $\pm l$, with the restriction $h + k + l = 3n$ for the rhombohedral centering of the cell. No absorption corrections were necessary.

Data reduction and structure refinement were performed using the SHELXTL[1] package of programs. Atomic coordinates of the known boron sites obtained from Callmer (*4*) were used as a starting point for the refinement with the additional boron sites being identified upon examination of a difference map. All partial occupancies were allowed to refine. In the final stages of refinement, a weighting function

$$w^{-1} = \sigma^2(F) + gF^2 \qquad (1)$$

was employed, where g was allowed to refine. The function minimized in the least-squares refinement was:

$$G(F) = \Sigma\, w(|F_o| - |F_c|)^2. \qquad (2)$$

The resulting R and weighted R values along with additional experimental details can be found in Table II.

A comparison of the observed and calculated structure factors for the 1775 unique observed reflections in sample EP is given in Appendix I.[2] The results for the other two samples were similar.

The atomic coordinates are given in Table III where the entries are x, y, z defined as:

$$x = 10^4(x_o/a_o), \quad y = 10^4(y_o/a_o), \quad z = 10^4(z_o/c_o).$$

Here a_o and c_o are the lattice parameters of the hexagonal unit cell and x_o, y_o, z_o are the position coordinates of a particular boron atom in the cell. Table III also gives the actual or equivalent isotropic thermal pa-

[1] G. Sheldrick, 1983, University of Göttingen, FRG, distributed through Nicolet Instrument Corp.

[2] See NAPS Document No. 04603 for 5 pages of supplementary materials from ASIS/NAPS, Microfiche Publications, P.O. Box 3513, Grand Central Station, New York, 10163. Remit in advance $4.00 for microfiche copy or for photocopy, $7.75 up to 20 pages plus $.30 for each additional page. All orders must be prepaid.

TABLE II

STRUCTURE DETERMINATION DETAILS FOR β-BORON SAMPLES

	Sample		
	MG57	EP	MG179
Scan range (2θ)	4–55°	4–80°	4–80°
Scan technique	$\omega/2\theta$	$\theta/2\theta$	$\theta/2\theta$
Number of reflections measured	3961	7507	6516
Number of unique reflections	735	1913	1894
Number of unique observed reflections	674	1775	1765
Cutoff criterion for observed reflections	$F > 4\sigma(F)$	$F > 3\sigma(F)$	$F > 3\sigma(F)$
Number of parameters refined	63	127	128
R	4.4	4.1	3.7
R (weighted)	4.9	4.8	5.5
Refined $g \times 10^5$	15	25	55
Maximum residual (% boron)	3.2	2.1	3.9
Crystal cooling rate	F	?	S

rameters, U, and the percentage occupancies, P, for sample EP. The atoms B1 through B16 in sample EP were refined with the anisotropic thermal parameters given in Appendix II.[2] The average trace of the U_{ij} matrix appears in Table III. The atoms B17 through B20 were refined with an isotropic U value. The errors listed for x, y, z, U, P, and the interatomic distances are one standard deviation.

TABLE III

COORDINATES OF BORON ATOMS IN THE HEXAGONAL UNIT CELL, SAMPLE EP

Atom	Site	x	y	z	U	P Percentage occupancy
B1	36i	1730(1)	1741(1)	1767(1)	6(1)*	100
B2	36i	3191(1)	2957(1)	1294(1)	6(1)*	100
B2	36i	2614(1)	2175(1)	4197(1)	6(1)*	100
B4	36i	2349(1)	2516(1)	3469(1)	6(1)*	100
B5	18h	545(1)	2x	9437(1)	5(1)*	100
B6	18h	865(1)	2x	132(1)	5(1)*	100
B7	18h	1098(1)	2x	8860(1)	5(1)*	100
B8	18h	1705(1)	2x	280(1)	5(1)*	100
B9	18h	1287(1)	2x	7666(1)	5(1)*	100
B10	18h	1020(1)	2x	6985(1)	5(1)*	100
B11	18h	564(1)	2x	3266(1)	5(1)*	100
B12	18h	897(1)	2x	3990(1)	5(1)*	100
B13	18h	579(1)	2x	5538(1)	11(1)*	74.5(6)
B14	6c	0	0	3855(1)	5(1)*	100
B15	3b	0	0	5000	14(1)*	100
B16	18h	546(2)	2x	1176(1)	9(1)*	27.2(7)
B17	18h	833(14)	2x	4760(11)	43(8)	8.5(9)
B18	18h	1440(7)	2x	5239(5)	6(3)	6.6(6)
B19	18h	1805(7)	2x	5347(5)	6(3)	6.8(6)
B20	36i	2067(21)	2280(22)	711(8)	11(4)	3.7(4)

Note. Asterisk indicates anisotropic when refined; no asterisk means an isotropic U was employed.

No corrections were made for absorption or extinction. The linear absorption coefficient of boron for Mo$K\alpha$ radiation is $\mu \cong 0.9$ cm^{-1}. Thus the small crystal size and the low atomic mass make these corrections unnecessary.

III. X-Ray Results

For sample EP the boron positions are given in Table III. For samples MG57 and MG179 the fully occupied boron sites were identical; the results for the partially occupied sites were not, and these are listed in Tables IV and V. The partially occupied site occupation depends somewhat on the preparation conditions and the cooling rate from the melting temperature. Note that the numbering scheme for the boron atoms is the same as that used by Hoard *et al.* (*2*) and Callmer (*4*). The main features of the structure are the same as those found by these previous authors. However, there is a slight difference in the positions of B8 and

TABLE IV

COORDINATES OF PARTIALLY OCCUPIED BORON ATOMS IN THE HEXAGONAL UNIT CELL

Sample	Atom	x	y	z	U^a
MG57	B13	583(2)	$2x$	5536(2)	11(1)
	B16	551(6)	$2x$	1169(4)	5(3)
	B17d	495(61)	1660(71)	4789(26)	4(16)
	B18	1421(31)	$2x$	5202(23)	8(16)
	B19	1780(17)	$2x$	5329(12)	0(11)
	B20	Vacant			
MG179	B13	580(1)	$2x$	5538(1)	10(1)
	B16	551(2)	$2x$	1176(1)	10(1)
	B17	841(8)	$2x$	4743(5)	66(10)
	B18	1458(7)	$2x$	5240(4)	12(4)
	B19	1801(5)	$2x$	5349(4)	2(2)
	B20	2010(50)	2250(50)	700(20)	[b]

[a] Isotropic U values were employed.
[b] The B20 position for MG179 was not refined, the errors are estimates. The B20 atom position is close to J_4 in Table VIII.

B16, which lies outside the experimental uncertainty. The main difference lies in the appearance of atoms B17, B18, B19, and B20. Table VI gives their distances from other boron atoms in the structure. These sites are all partially occupied, with percentage occupancies between 3.2 and 9.7%, as given in Table V. Other possible boron sites have occupancies which are less than 3% of a boron atom.

TABLE V

PERCENTAGE OCCUPANCIES, P, OF PARTIALLY OCCUPIED BORON SITES AND X-RAY VALUES OF N_B

	Measured P			Calculated P		
Site	MG57	EP	MG179	MG57	EP	MG179
B13	77.7(14)	74.5(6)	73.0(5)	77.7[a]	74.5[a]	73.0[a]
B16	25.8(13)	27.2(7)	28.4(5)	?	?	?
B17	—	8.5(9)	9.7(7)	0.00	8.83	10.33
B17d	3.2(8)	—	—	2.82	—	—
B18	5.8(15)	6.6(6)	7.4(6)	5.63	8.83	10.33
B19	7.2(14)	6.8(5)	7.0(5)	11.03	7.83	6.33
B20	0	3.7(4)	2.5(25)	5.52	3.92	3.17
Σ_1	97.1(72)	96.4(27)	97.1(28)	100[a]	100[a]	100[a]
$N_B(X)$	319.1(15)	320.6(7)	319.6(6)	—	—	—

[a] Assumed value for the calculation.

Bonding of Partially Occupied Sites

The partially occupied boron sites in the structure are listed in Tables IV and V. These are illustrated in Fig. 2 where it can be seen that these partially occupied sites all occur close to a line joining the fully occupied B15 site with the A_1 vacant position. Except for position B20 they all lie in the same $(1\bar{2}10)$ plane.

If we consider the β-boron structure to be made up of B_{12} and B_{28} clusters of atoms and one B15 atom which constitutes the basic framework, then B13 is a partially vacant framework site, while B16, B17, B19, and B20 are partially occupied interstitial sites. An analysis of Fig. 2 suggests that the framework region adjacent to the A_1, A_2,

TABLE VI

BOND LENGTHS IN Å FOR BORON ATOMS B16, B17, B18, B19, AND B20

Bond	EP	MG57	MG179
B16–2B1	1.801(6)	1.809(13)	1.797(6)
–2B5	1.787(6)	1.778(13)	1.791(6)
–2B7	1.802(6)	1.805(9)	1.800(5)
–2B16	1.791(7)	1.808(15)	1.805(7)
– B19	1.891(15)	1.938(33)	1.888(12)
– B20	1.875(19)	—	1.84(7)[a]
B17– B12	1.837(26)	1.939(62)	1.792(13)
– B13D	1.570(15)	1.840(85)	1.562(12)
– B13E	1.570(15)	1.409(53)	1.562(12)
– B13A	1.913(26)	1.873(65)	1.956(13)
– B15	1.678(10)	1.690(75)	1.706(7)
– B18	1.618(30)	1.977(77)	1.663(19)
B18–2B3	1.664(16)	1.727(47)	1.666(10)
–1B13	1.778(15)	1.773(58)	1.807(14)
B19–2B1	1.890(12)	1.897(28)	1.897(10)
–2B2	1.875(6)	1.878(10)	1.874(6)
–2B3	1.723(18)	1.722(26)	1.713(9)
– B20	1.915(22)		Present[a]
B20– B2	1.752(19)	None	Present[a]
– B3	1.718(21)		
– B5	1.684(6)		
– B6	1.789(20)		
– B7	1.707(16)		
– B8	1.797(18)		

[a] Not refined.

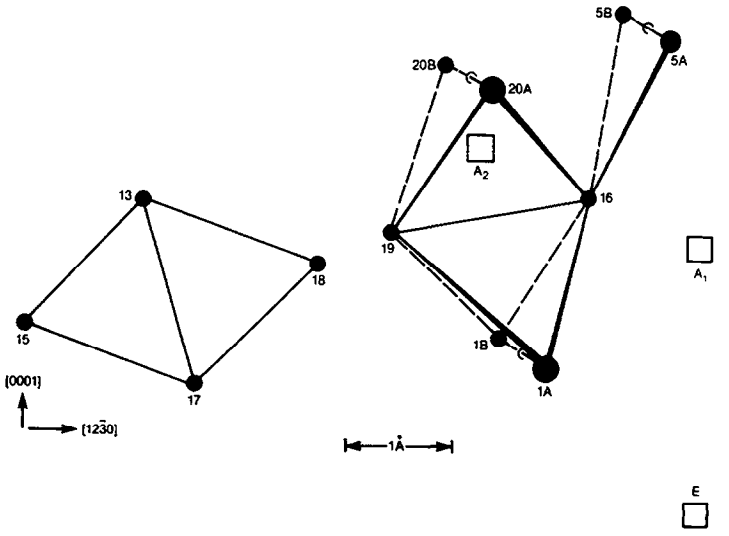

FIG. 2. The relative positions of the partially occupied boron sites (13, 16, 17, 18, 19, 20) with respect to the framework sites (1, 5, 15) in β-boron. The open squares are the centers of the vacant regions in the crystal designated as A_1, A_2, E.

and E vacancies attracts interstitial boron atoms, while the region around B13 and B15 donates boron atoms to create partially vacant B13 sites. Thus Fig. 2 represents the region of the crystal in which the framework readjusts the local atomic density.

In Fig. 3 we show the local environment of the B17 and B18 sites with more detail than in Fig. 2. The B17 and B18 atoms have almost (to within 25%) the same fractional occupancies; thus it is suggested here that they almost always occur in pairs. Such a linked pair is shown in Fig. 3 where B12, B13A, B15, B17, and B18 lie in the same $(1\bar{2}10)$ plane all close to B15. Note that B15 is at the center $(0, 0, \frac{1}{2})$ of the hexagonal unit cell. With the arrangement in Fig. 3 both B17 and B18 are bonded to each other and then to only three other boron atoms. It can be seen that the center of B17 is only 1.572 Å away from boron positions B13E and B13D. Such a distance is too short for a boron–boron bond. Thus we believe that B17 is only occupied when both B13E and B13D are vacant.

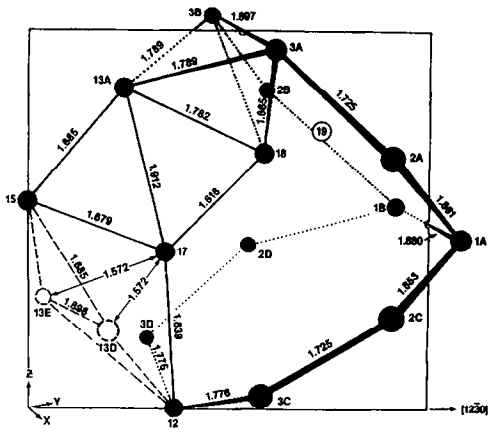

FIG. 3. The local environment of a B17 plus B18 pair in β-boron. The sites B13D and B13E are vacant because of their proximity to an occupied B17 site. B19 is also shown as vacant.

Furthermore, we suggest that when B13E and B13D are both occupied, the neighboring B17 position must be vacant. In such a case a boron atom in the B18 position is in an unstable configuration, with only three possible bonds. Furthermore, if B13A is vacant then only two bonds are possible. In order to increase its bonding, the B18 atom then moves to the

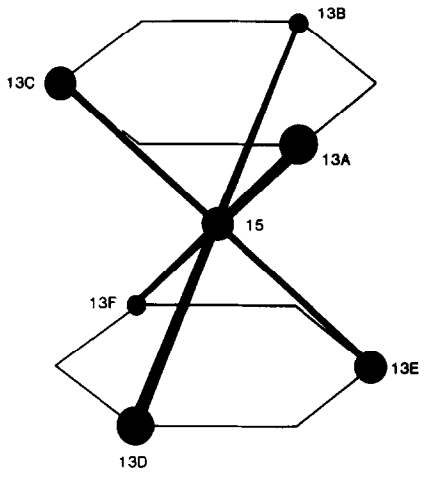

FIG. 4. The six B13 sites surrounding a B15 site at the center of the unit cell of β-boron.

B19 position where it is now bonded to the fully occupied 2B1 + 2B2 + 2B3 atoms at distances of 1.72 to 1.89 Å. This means that neighboring positions B18 and B19, which are 0.72 Å apart, are never simultaneously occupied.

IV. Model Computations of Partial Occupanies

From Table V we see that B13 is only 74.5% occupied in sample EP. The B13 positions are situated on a triangular antiprism around atom B15 as shown in Fig. 4. Let us suppose that either one or two of these six B13 atoms are missing around various B15 sites. The average number of B13 neighbors of a B15 is 4.47 atoms. Thus 53% of the time there will be four neighbors and 47% of the time there will be five neighbors. Furthermore, let us suppose that when there are only five neighbors B13A is vacant and B19 atom, as in Fig. 3, is present. The probability that only one B13 site is vacant times the probability that this vacant site is adjacent to a B19 site is:

$$\frac{P(19)}{100} = (0.470) \times (0.1667) = 0.0783. \quad (3)$$

Thus 7.83% is the estimated percentage occupancy of B19.

In the case where two B13 sites are vacant, let us suppose they always occur as pairs either in the A–B–C ring in Fig. 4 or in the D–E–F ring, but not as one vacancy in each ring simultaneously. Then the probability of having a divacancy times the probability of it being adjacent to a B17–B18 pair is:

$$\frac{P(17)}{100} = \frac{P(18)}{100} = (0.530) \times (0.1667) = 0.0883. \quad (4)$$

By this method we obtain the calculated percentage occupancies for samples EP and MG179 in Table V. For MG179 we calculate a larger $P(17) = 0.1033$ because $P(13)$ is less than for sample EP. Note that they are close to the observed values.

This model suggests that one B19 is always occupied whenever only one B13 is vacant, and a B17–B18 pair is always occupied whenever two B13 positions are vacant. If this is true, then the sum, Σ_1, of the percentage occupancies, P_i, should be 100%. From Table V note that:

$$\Sigma_1 = P(13) + P(17) + P(18) + P(19) = 96.4(27)\% \text{ for EP.} \quad (5)$$

The result is 100% to within the uncertainty of the measurement. It is almost as if the boron atoms that should have been in the B13 site in the framework have been displaced but not lost to the structure.

For the calculated occupancies in sample MG57 we have used a slightly different approach. For $P(19)$ we use Eq. (3) to obtain:

$$\frac{P(19)}{100} = (0.6620) \times (0.1667) = 0.1103.$$

Then we calculated $P(17d)$ and $P(18)$ by assuming that:

$$\Sigma_1 = P(13) + 2P(17d) + P(18) + P(19) = 100\% \quad (6)$$

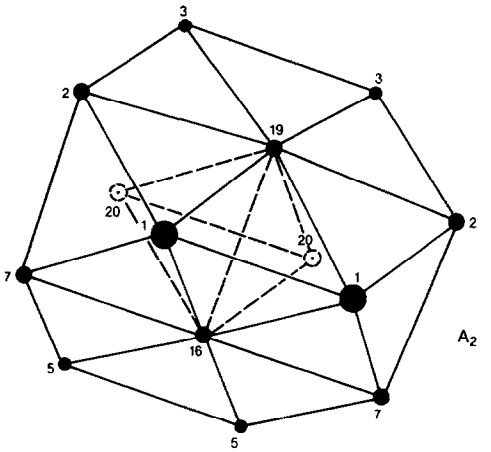

FIG. 5. The truncated tetrahedron which forms the walls of the vacant A_2 site in β-boron. The vertices 1, 2, 3, etc., are fully occupied by boron atoms. The partially occupied boron sites B16, B19, and B20 are located very near to the centers of the four planar, hexagonal faces of the figure. Their mutual bonds form an internal tetrahedron shown by the dashed lines. Atoms B6 and B8 which form part of the truncated tetrahedron are not shown. Atom B6 lies beneath B16 and atom B8 lies beneath B19, both on the underside of the truncated tetrahedron.

and

$$2P(17d) = P(18).$$

This means that we have assumed B17d always occurs as a pair with B18 and that any boron atoms lost from B13 positions always end up as B17d–B18 pairs or B19 singles. The number of theoretically possible B17d positions corresponding to only one B13 vacancy is much greater than the number from the above calculation. So the concentration of B17d atoms actually found is limited not by the available sites, but rather by the availability of boron atoms displaced from B13 positions.

Computation for B16, B19, and B20

As shown in Fig. 2, the four positions B16 + B19 + 2B20 form a tetrahedron. This tetrahedron has the same center as the A_2 interstitial vacancy. In fact the walls of the A_2 vacancy are in the form of a truncated tetrahedron which has 12 vertices at fully occupied boron framework atoms (2B1 + 2B2 + 2B3 + 2B5 + 1B6 + 2B7 + 1B8). This is shown in Fig. 5. The walls consist of 4 nearly perfect, planar hexagons and four nearly equilateral triangles. The B16, B19, and B20 sites are located very close to the centers of the hexagonal faces.

The following suggestion is offered as a tentative model for the occupancies of these three sites. Since there are more filled B16 sites per unit cell than either B19 or B20, we postulate that B19 or B20 sites are only occupied when they are adjacent to an occupied B16 sites. This explains why, in impurity-doped samples, no occupation of B19 or B20 is seen when the B16 occupancy decreases. Furthermore, we postulate that occupied B19–B20 boron sites occur only in pairs. This is based on the observation that:

$$P(B19) \simeq 2P(B20) \qquad (7)$$

and that there are twice as many B20 sites (36i) per unit cell as there are B19 sites (18h). With this model we expect that of the 18 tetrahedra around the A_2 centers in a hexagonal unit cell we will find 13 empty, 4 with only B16 atoms, and 1 with a triplet of 1B16 + 1B19 + 1B20.

V. Crystal Density

Measurements

The flotation density and X-ray lattice parameters of a number of different boron crystals were measured in order to obtain values for the number of boron atoms in a unit cell. The results are given in Table VII. We have measured natural boron which is a mixture of B^{10} and B^{11} isotopes as well as enriched B^{10} and enriched B^{11} samples. The relative isotopic abundances of B^{10} and B^{11} in all of the samples was measured with the use of a mass spectrometer (at Isotopic Analysis, Tulsa, OK). This precaution was

TABLE VII

DENSITIES AND HEXAGONAL CELL PARAMETERS FOR VARIOUS β-RHOMBOHEDRAL BORON SAMPLES

V (Å^3)	Sample No. and cooling rate	B^{10} atom%	M (g)	Density (g/cm^3)	a_0 (Å)	c_0 (Å)	N_B (D)
2464.9(10)	MG77, F	98.45(5)	10.0283(5)	2.157(2)	10.932(1)	23.818(3)	319.4(4)
2463.8(9)	MG57, F	20.07(5)	10.8093(5)	2.337(2)	10.930(1)	23.815(3)	320.8(4)
2463.9(9)	MG79, F	1.49(5)	10.9945(5)	2.373(2)	10.930(1)	23.815(3)	320.3(4)
2461.2(9)	MG179, S	20.07(5)	10.8093(5)	2.332(2)	10.925(1)	23.810(3)	319.7(4)
2465.3(20)	Eagle Picher	20.07(5)	10.8093(5)	2.333(2)	10.932(2)	23.819(5)	320.4(5)
?	Hoard *et al.* (*2*)		10.809	2.35			
?	Holcombe *et al.* (*11*)		10.809	2.326			
?	King *et al.* (*12*)		10.809	2.345(5)			
?	Slack *et al.* (*7*)		10.8090(5)	2.329(5)			
		20.10(5)					

needed because different boron sources can have different isotopic abundance ratios.

The samples MG57, MG77, MG79, and MG179 were grown from the melt in CVD boron nitride crucibles. Their nitrogen content after growth was measured as 250 ppm by weight (193 atomic ppm). The possible effect of this amount of nitrogen on the measured density is not detectable by our X-ray or pycnometric methods whether it is substitutional or interstitial.

For samples MG57, 77, 179, and EP the lattice constants were measured on powdered samples using a Guinier X-ray camera with Cu$K\alpha_1$ radiation and a silicon-powder standard. We note that the lattice constants of the B^{10} and B^{11} samples are almost identical, but their densities are distinctly different. For all of the present samples in Table VII, the flotation density combined with a_0 and c_0 values from the X-ray work give

$$N_B(D) = 320.1(4)$$

as the average number of boron atoms per hexagonal unit cell. The single-crystal X-ray studies on samples EP and MG179 with the Nicolet diffractometer gives an average X-ray value for $N_B(X)$ of:

$$N_B(X) = 320.1(5).$$

This is in excellent agreement with $N_B(D)$ and indicates that there are no undiscovered, partially occupied boron sites in the lattice with $P \geq 1\%$.

The present density measurements are compared in Table VII with previous values from the literature (*2*, *6–8*).

Vacant Sites

A description of the vacant positions such as A_1, A_2, A_3, E, and D in the β-boron structure has been given by Andersson and Lundström (*9*) and by Sullenger (*10*). We have recalculated the ideal positions for the A_1, A_2, and A_3 interstitial sites. These three sites all have walls which are truncated tetrahedra with four nearly perfect planar hexagonal faces. These face-center positions have also been calculated; the results are in Table VIII. The ideal positions (x, y, z) of the centers have been calculated from:

$$nx = \sum_{i=1}^{n} x_i, \quad ny = \sum_{i=1}^{n} y_i, \quad nz = \sum_{i=1}^{n} z_i \quad (8)$$

where the x_i, y_i, z_i are the coordinates of the 6 or 12 framework boron atoms surrounding the sites. Thus, $n = 6$ or 12. We have found (*11*) that impurities can enter the A_1 or A_2 sites (*9*), but that only three of the possible seven facial sites, J_i, are par-

TABLE VIII

IDEAL COORDINATES OF THE CENTERS OF THE A_1, A_2, A_3 SITES AND OF THEIR HEXAGONAL FACES

Site	Occupied by	Position	x	y	z	Framework boron neighbors
A_1	Dopant atoms	6c	0	0	1309	6B1 + 3B5 + 3B7
A_2	Dopant atoms	18h	1080	$2x$	972	1 + 1 + 2 + 2 + 3 + 3 + 5 + 5 + 6 + 7 + 7 + 8
A_3	0	36i	2801	2378	431	2 + 3 + 4 + 4 + 5 + 6 + 6 + 7 + 8 + 8 + 9 + 10
J_1	0	6c	0	0	1767	1 + 1 + 1 + 1 + 1 + 1
J_2	B16	18h	564	$2x$	1157	1 + 1 + 5 + 5 + 7 + 7
J_3	B19	18h	1458	$2x$	1308	1 + 1 + 2 + 2 + 3 + 3
J_4	B20	36i	1990	2299	712	2 + 3 + 5 + 6 + 7 + 8
J_5	0	18f	2588	2588	0	4 + 4 + 6 + 6 + 8 + 8
J_6	0	18h	2857	1429	435	5 + 6 + 7 + 8 + 9 + 10
J_7	0	36i	3770	3198	579	2 + 3 + 4 + 4 + 9 + 10

tially populated by boron atoms. It may be possible that boron atoms can partially occupy the vacant facial sites, J_1, J_5, J_6, or J_7, under some conditions. In our three samples these occupancies must be very low because of the good agreement between $N_B(D)$ and $N_B(X)$.

Internal Densities

The structure of β-boron has been previously described by Hoard *et al.* (*2*) as composed of B_{84}, B_{10}, and B_1 units, with the B_{84} unit containing 1 icosahedron and 12 half-icosahedra for a total of 84 boron atoms. This is described in Fig. 2 of Hoard *et al.* (*2*). The center of this B_{84} unit is the center of the 6B5 + 6B6 icosahedron and has x, y, z coordinates of 0, 0, 0. A hypothetical sphere of radius 5.241 Å will just enclose all 84 boron atoms. Within such a sphere are all of the sites A_i or J_i listed in Table VIII as well as the B18 sites. Thus such a sphere contains 86.88 boron atoms. A hexagonal unit cell contains three such spheres. There is a small overlap between these spheres. If we correct the B_{84} volume for this very small overlap effect (−0.46%), the local density *within* the spherical B_{84} regions is 2.598 g/cm^3. Such regions make up 73% of the volume of the unit cell. The rest of the unit cell volume occupied by atoms B11, B12, B13, B14, B15, and B17 has a local density of 1.611 g/cm^3.

The packing density, ϕ, is defined (*12*) as the fraction of the total volume actually occupied by boron atoms, which are assumed to be spheres. If we use an average spherical radius of 0.88 Å for boron, then the B_{84} regions have $\phi = 0.413$. The remainder has $\phi = 0.267$. It can be seen (*12*) that a ϕ of 0.413 is rather common for a coordination number, η, of $\eta = 6$. However, a ϕ of 0.267 is very low and has not been found (*12*) in any common structure with $\eta = 6$. The weighted average coordination number of the B11 to B17 collection is $\eta = 5.87$.

In Fig. 2, the partially occupied sites are shown to be concentrated near the A_2 vacancy position. Now we can see that the partially occupied sites are contributing to increasing the packing density, ϕ, of the B_{84} units, somewhat at the expense of the rest of the unit cell. The extra boron atoms in these partially occupied sites of B_{84} actually increase the local density by 3.4%. Without them the local density would have been 2.512 g/cm^3.

VI. Excess Electron Density

The structure refinement has been carried out for sample MG57 using 19 boron

TABLE IX
EXCESS ELECTRON DENSITY NEAR THE CENTERS OF THE INTERCLUSTER BONDS

Bond center	Position at center	Peak electron density (e/Å^3) MG57	EP	MG179
B1–B1	18h	0.28	0.36	0.38
B2–B3	36i	0.38	0.46	0.35
B4–B4	18f	0.37	0.39	0.43
B5–B7	18h	0.32	0.42	0.42
B6–B8	18h	0.38	0.49	0.49
B9–B10	18h	0.36	0.37	0.36
B13–B15	18h	0.27	0.29	<0.26

positions and for samples EP and MG179 using 20 boron positions. After the structure has been thus refined assuming spherical boron atoms a difference electron density map was computed. This map shows that there is excess electron density accumulated near the centers of the intercluster bonds. The identification of these clusters of B_{12} and B_{28} groups and the intercluster bonds is given by Slack *et al.* (*11*). The magnitude of this excess gives peaks in the electron density of 0.3 to 0.5 e/Å^3 for all of the intercluster bonds. The results are listed in Table IX. Note that all three samples have very similar residuals.

If all of this residual electron density were incorrectly attributed to boron atoms actually being located at the centers of these bonds with a small partial occupancy of 2 to 3% of a boron atom, then the total excess electron density would amount to at least four extra boron atoms per hexagonal unit cell. The agreement between $N_B(X)$ and $N_B(D)$ is too good, i.e., ±0.2 (Eagle Picher Laboratories) boron atoms/cell, for four atoms per cell to be unaccounted for. The electron density peaks near the intercluster bond centers are just electron accumulation, not boron atoms. A similar electron concentration at intericosahedral bonds has also been found in α-boron crystals by Will *et al.* (*13*) using a more sophisticated analysis.

VII. Previous Studies of Partial Occupancies

As mentioned previously, the sites B17, B18, B19, and B20 have not previously been reported as being occupied by boron atoms. However these positions were reported as being partially occupied either by Ge or by Ni atoms in studies by Lundström *et al.* (*14, 15*). Thus we make the identification in Table X of Ni(4) and Ge(7) with B17d and Ni(3) and Ge(5) with B18. We have converted the reported percentage occupancies to the equivalent number of boron atoms by multiplying by the ratios of the atomic number of Ni (or Ge) to that of boron. We see that both the atom positions and occupancies are compatible with the reidentification as boron atoms. This reidentification makes some of the metal–boron bond lengths originally given for these Ni and Ge sites much more compatible with normal boron–boron distances.

TABLE X
OCCUPIED B17 OR B18 POSITIONS REPORTED IN THE LITERATURE

Ref.	Notation	x	y	z	Position	P (%)
(*14*)	Ge(7)	480(20)	1650(10)	4745(6)	36i	2.7
(*15*)	Ni(4)	617(6)	1744(6)	4753(2)	36i	3.2
This work	B17d	495(61)	1660(71)	4750(10)	36i	3.2
(*14*)	Ge(5)	1423(9)	$2x$	5220(7)	18h	6.6
(*15*)	Ni(3)	1497(6)	$2x$	5223(2)	18h	10.0
This work	B18	1450(10)	$2x$	5240(5)	18h	6.6

Furthermore, we have actually found boron atoms in the B17, B17d, or B18 sites in a number of other samples doped with various transition elements (*11*).

VIII. Conclusions

We have found four new boron atom positions in the unit cell of β-boron. The number of atoms in the unit cell is now fixed at 320, both from flotation density and X-ray studies. If the atomic mass is 10.809 g/mole then the crystal density is 2.333 g/cm^3 for crystals cooled slowly from the melt. There are density variations within the large unit cell, and the higher density regions have enhanced density caused, in part, by boron atoms in partially occupied interstitial positions.

Acknowledgment

We wish to thank W. W. Knapp for growing many of the boron crystals used in this study.

References

1. R. E. Hughes, C. H. L. Kennard, K. G. Sullenger, H. A. Weakliem, D. E. Sands, and J. L. Hoard, *J. Amer. Chem. Soc.* **85,** 361 (1963).
2. J. L. Hoard, D. B. Sullenger, C. H. L. Kennard, and R. E. Hughes, *J. Solid State Chem.* **1,** 268 (1970).
3. D. Geist, R. Kloss, and H. Follner, *Acta Crystallogr.* **26,** 1800 (1970).
4. B. Callmer, *Acta Crystallogr. Sect. B* **33,** 1951 (1977).
5. J. Cueilleron, J. C. Viala, F. Thevenot, C. Brodhag, J. M. Dusseau, and A. El Biach, *J. Less-Common. Met.* **59,** 27 (1978).
6. G. A. Slack, D. W. Oliver, and F. H. Horn, *Phys. Rev. B* **4,** 1714 (1971).
7. C. E. Holcombe, D. D. Smith, J. D. Lore, W. K. Duerksen, and D. A. Carpenter, *High Temp. Sci.* **5,** 349 (1973).
8. I. R. King, G. R. Taylor, F. E. Wawner, and C. P. Talley, Aeronaut. Sys. Divis., Wright-Patterson Air Force Base Tech. Doc. Report 62-427 (Jan. 1963).
9. S. Andersson and T. Lundström, *J. Solid State Chem.* **2,** 603 (1970).
10. D. Sullenger, Ph.D. Thesis, Cornell University, Ithaca, NY (1969).
11. G. A. Slack, C. Hejna, M. Garbauskas, and J. S. Kasper, *J. Solid State Chem.* **76,** 64 (1988).
12. G. A. Slack, *Z. Kristallogr.* **165,** 1 (1983).
13. G. Will, B. Kiefer, B. Morosin, and G. A. Slack, "Novel Refractory Semiconductors" (T. Aselage *et al.*, Eds.), *Proc. Mater. Res. Soc.* **7,** xx (1987).
14. T. Lundström and L. E. Tergenius, *J. Less-Common Met.* **82,** 341 (1981).
15. T. Lundström, L. E. Tergenius, and I. Higashi, *Z. Kristallogr.* **167,** 235 (1984).